(^{3}He, t) Reactions on ^{54}Fe, ^{58}Ni, and ^{60}Ni[†]

H. Rudolph* and R. L. McGrath

Department of Physics, State University of New York, Stony Brook, New York 11790

(Received 20 February 1973)

(^{3}He, t) differential cross sections on ^{54}Fe, ^{58}Ni, and ^{60}Ni targets have been studied at 24-MeV incident energy. Triton angular-distribution systematics are suggested by corroborative data from other work. On this basis several tentative spin-parity assignments in the copper isotopes are given. Distorted-wave Born-approximation calculations based on a microscopic effective-interaction model are presented for ^{54}Fe and ^{58}Ni. These are in fair agreement with the data for the ^{54}Co states thought to have $(1f_{7/2})^{-2}$ structure, and for the $T=1$ ^{58}Cu states. However, these calculations generally do not yield consistent effective-interaction strengths or correct angular-distribution shapes for the $T=0$ ^{58}Cu transitions. Simple two-particle wave functions are used for mass-58 states where the nucleons occupy the $2p_{3/2}$, $1f_{5/2}$, or $2p_{1/2}$ orbitals.

I. INTRODUCTION

For several years investigations have shown that the (^{3}He, t) reaction can be useful in nuclear spectroscopy. In some cases, triton angular distributions have exhibited systematic behavior depending upon the angular momentum transfer and parity change in the reaction.[1-6] Distorted-wave calculations based on a microscopic model of the effective nucleon interaction have been semiquantitatively successful in the $1p$ and $1f$ shell.[7-9] These analyses usually are based on a phenomenologicalistic static potential composed of a central term including spin and charge-exchange operators plus a tensor term related to the one-pion-exchange (OPEP) form.

The present spectroscopic studies of ^{58}Cu and ^{60}Cu were initiated with the hope of establishing spins and parities from data systematics. In addition, available wave functions, where the valence nucleons are distributed in the $2p_{3/2}$, $1f_{5/2}$, and $2p_{1/2}$ orbitals with ^{56}Ni acting as a closed core, were to be tested using the microscopic distorted-wave model. The empirical strengths of various terms in the effective interaction at 24-MeV incident energy were to be determined by analysis of the ^{54}Fe(^{3}He, t)^{54}Co reaction assuming pure $(f_{7/2})^{-2}$ configurations for ^{54}Fe and the strongly populated states of ^{54}Co. While some of these goals were achieved, the more complicated spin-flip transitions to unnatural-parity states in ^{58}Cu could not be fitted within this microscopic framework. The structure calculations[10] for ^{60}Cu, which include only seniority zero and two states, do not reproduce the observed level ordering or density and therefore no reaction calculations were done for the ^{60}Ni(^{3}He, t)^{60}Cu reaction. Nevertheless, some spin-parity assignments are suggested by the systematic triton angular-distribution shapes in conjunction with a previous[11] ^{58}Ni(^{3}He, p)^{60}Cu study.

II. EXPERIMENTAL METHODS

Data were collected at 24-MeV incident ^{3}He energy with two three-counter telescopes. The first two detectors were operated in a ΔE-E mode for particle identification using standard techniques, while the third detector was used to veto longer-range protons and deuterons. All three targets were rolled metallic foils. The nickel targets were 300 μg/cm^2 thick with isotopic purity $\geq 99.5\%$, while the ^{54}Fe target was 900 μg/cm^2 thick and greater than 96% isotopically pure. Examples of triton energy spectra are shown in Figs. 1-3. The energy resolution for the nickel targets was 40–60 keV full width at half maximum (FWHM) and 70–80 keV FWHM for the ^{54}Fe target. In general the data were taken in two- or four-degree steps from 10 to 80° laboratory angle. Ab-
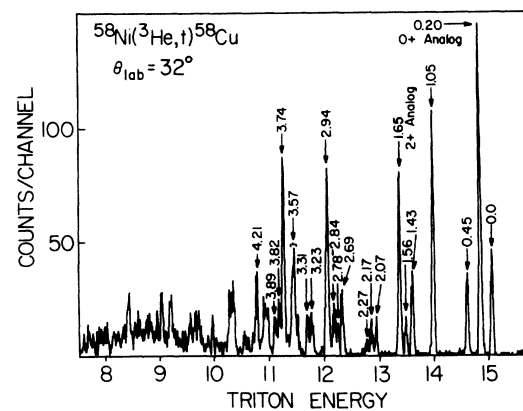

FIG. 1. A ^{58}Ni(^{3}He, t)^{58}Cu energy spectrum at $E_{^3\text{He}}$ = 24 MeV. The energy resolution is 40 keV (FWHM).
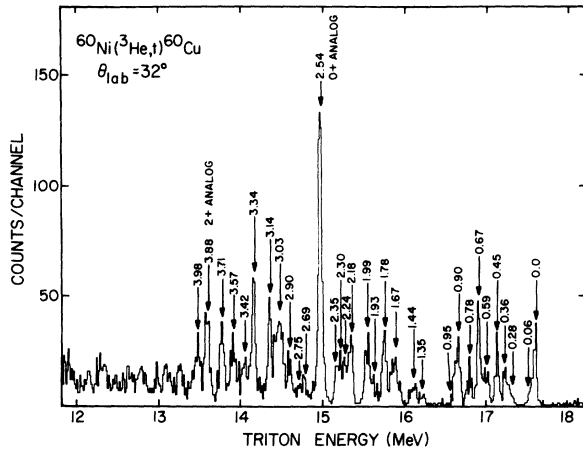
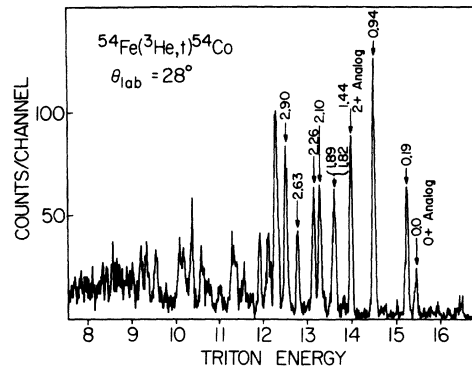FIG. 2. A ^{60}Ni(^{3}He, t)^{60}Cu energy spectrum. The energy resolution is 45 keV (FWHM).

FIG. 3. An ^{54}Fe(^{3}He, t)^{54}Co energy spectrum. The energy resolution is 70 keV (FWHM).

solute angle measurements were estimated accurate to ±0.2° and checked by Rutherford scattering and by comparison of the elastic scattering of 23.9-MeV ^{3}He ions from ^{12}C to the data of Warshaw et al.[12] In order to obtain absolute cross sections, ^{3}He elastic scattering from each target was measured at 10-MeV incident energy for laboratory angles between 10 and 15° compared to

the Rutherford scattering formula. The probable uncertainty in this normalization is ±15%. Excitation energies of states found in this experiment were obtained by comparison with levels observed in the ^{27}Al(^{3}He, t)^{27}Si reaction, and in some cases from (p, $n\gamma$) Ge(Li) detector data.[13] (The latter data are consistent with recently published papers.[14, 15])

TABLE I. Excitation energies (MeV), L transfer [in the (^{3}He,t) reaction], and spin-parity assignments for states of ^{58}Cu.

	Present results		(p,n) [a]		(p,$n\gamma$) [b]	
0.0 [c]	(0 + 2)	1$^+$	0.0		0.0 [d]	
0.20	0	0$^+$, T = 1	0.209 ± 0.012	0$^+$, T = 1	0.203	
0.45	(2 + 4)	(3$^+$)	0.441 ± 0.013		0.445	2 or 3
1.05	(0 + 2)	(1$^+$)	1.043 ± 0.020		1.052	1
1.43	2	(2$^+$)			1.428	0→3
1.55					1.550	1→5
1.65	2	2$^+$, T = 1	1.638 ± 0.029		1.647	≤3
2.07					1.652	1→5
2.17						
2.27						
2.69	4	4$^+$, T = 1				
2.78						
2.84						
2.94	(4 + 6)	(5$^+$)				
3.23						
3.31						
3.57 [e]						
3.74						
3.82						
3.89						
4.21						

[a] Reference 16.
[b] References 14 and 15.
[c] Excitation uncertainties are ±10 keV for E_x <2 MeV, ±20 keV otherwise.
[d] Excitation uncertainties are approximately ±3 keV.
[e] Several states.

III. EXPERIMENTAL RESULTS

The triton energy spectrum from the ^{58}Ni(^{3}He, t)-^{58}Cu reaction (Fig. 1) is consistent with ($p, n\gamma$)[14, 15] and (p, n)[16] data for excitations less than 2 MeV. Most of the energy levels labeled in the ^{60}Ni(^{3}He, t)-^{60}Cu spectrum (Fig. 2) were observed by Young and Rapaport[11] using the ^{58}Ni(^{3}He, p)^{60}Cu reaction. The weakly populated 0.163-MeV state reported by them is not found in the present data. There is no evidence for γ decay to or from this state

in the ($p, n\gamma$) data.[13, 17] The energy level data are summarized in Tables I and II. Generally angular distributions were extracted for triton groups with reasonable statistics which apparently corresponded to single states at most angles. Consistent with these criteria, ^{58}Cu angular distributions were obtained for states below 2 MeV and ones at 2.69 and 2.94 MeV. Angular distributions were extracted from nine low-lying ^{60}Cu states.

The low-lying ^{54}Co states (Fig. 3) have been investigated several times via the (^{3}He, t) reac-

TABLE II. Excitation energies (MeV), L transfer, and spin-parity assignments for states of ^{60}Cu.

Present work			Previous (^{3}He,p) results [a]		
Energy [b]	L	J^π [c]	Energy [d]	L	J^π
0.0	2	2^+	0.0	2	2^+
0.06	(0+2)	1^+	0.058	0+2	1^+
			0.163		
			0.287	2	$(2)^+$
0.29					
0.36			0.361	0+2	1^+
0.45	(2+4)	(3^+)	0.452	(2+4)	$(3)^+$
0.56			0.558	(4)	$(4)^+$
0.60			0.597	(2+4)	$(3)^+$
0.67	(0+2)	(1^+)	0.667	(0+2)	$(1)^+$
0.78			0.779		
0.90	(2+4)	(3^+)	0.900		
0.95					
1.35					
1.44			1.659		
1.67 [e]			1.779	(0+2)	$(1)^+$
1.78	(0+2)	(1^+)	1.930 ± 20		
1.93			1.990		
1.99			2.179	(2)	$(2)^+$
2.18	(0+2)	$(1,2)^+$	2.242		
2.24			2.286		
2.30			2.356		
2.35			2.536	0	0^+
2.54	0	$0^+, T=2$	2.715		
2.69			2.763		
2.75			2.915	(0)	$(0)^+$
2.90			2.977	2	$(2)^+$
			3.072 ± 20		
3.03 [e]			3.137		
3.14			3.313		
3.34					
3.42			3.515		
3.57			3.698		
3.71			3.874	(2)	$(2)^+$
3.88	2	$2^+, T=2$			
3.98			4.619 ± 20		
			4.638 ± 20		

[a] Reference 11.

[b] Excitation uncertainties are ±10 keV for E_x <1 MeV, ±20 keV otherwise.

[c] J^π assignments combine present work with previous data where possible as discussed in text.

[d] Excitation uncertainties are ±10 keV for E_x <1 MeV and ±15 keV for states above 1 MeV unless otherwise indicated.

[e] Several states.

tion[1,5,18] and with the (p, n)[16] and $(p, n\gamma)$ reac-
tions.[15] The states presumed to correspond to the
$(f_{7/2})^{-1}{}_\pi (f_{7/2})^{-1}{}_\nu$ configuration are those labeled
at: 0.0, 0^+; 0.19, 7^+; 0.94, 1^+; 1.44, 2^+; 1.82,
(3^+); 2.10, (5^+); 2.63, 4^+; 2.90, (6^+).[19] Two weak-
ly excited states at 2.15 and 2.84 MeV were re-
solved by Schwartz, Sherr, and Bhatia[5] but not in
the present experiment. A state at 1.59 MeV ob-
served in low-energy (p, n) work[15] is not apparent
in these data. Angular distributions were ex-
tracted for all of the members of the $(f_{7/2})^{-2}$ multi-
plet. In order to determine the angular distribu-
tions for the 2.10-MeV state, it was necessary to

include the data for the 2.26-MeV state in the
analysis, and the angular distribution for this
state is included with those presented below.

Where possible, angular distributions have been
grouped together which have similar shapes.
These are shown in Figs. 4–11. J dependence
has previously been demonstrated only for states
with simple configurations, e.g., in ^{48}Sc,[1,3] ^{54}Co,[1]
and ^{90}Nb,[4] and there is no *a priori* reason to be-
lieve that the angular distributions for mixed con-
figuration states will show this same systematic
behavior. It appears, however, that many of the
angular distributions for states in ^{58}Cu and ^{60}Cu
also show systematic behavior which may be char-
acterized by the spin of the final state and some
spin assignments will be tentatively suggested on
this basis. The DWBA (distorted-wave Born-ap-
proximation) shapes shown for some transitions
are discussed below.

The natural-parity transitions are shown in
Figs. 4–7. The ground-state analog angular dis-
tributions shown in Fig. 4 are distinctively oscil-
latory with typical $L = 0$ shapes. Although two
other 0^+ states in ^{58}Cu and four 0^+ states in ^{60}Cu
are predicted within the range of excitation ener-
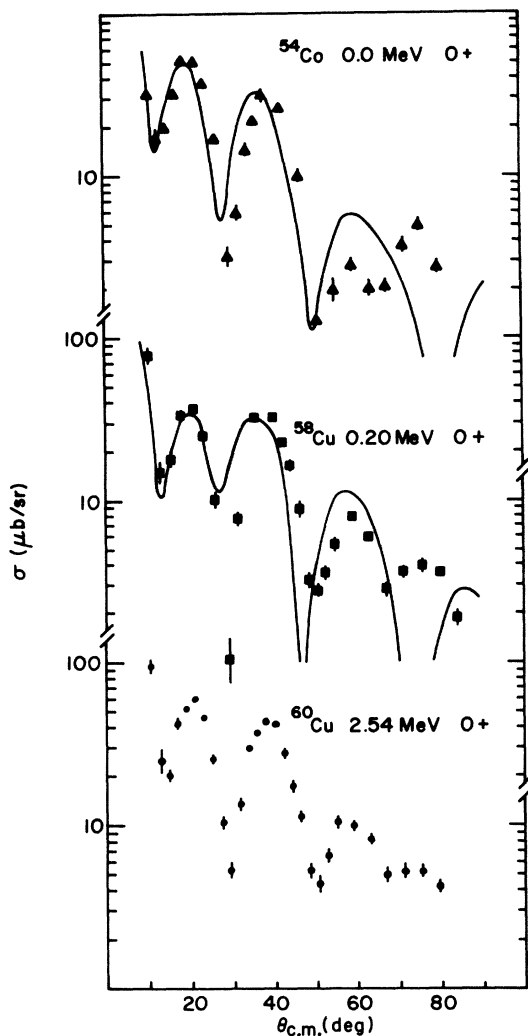gies studied, no other triton groups were observed

FIG. 4. $(^3$He, $t)$ angular distributions for the three 0^+
isobaric analog states observed in the present work. The
$L = 0$ curves come from the central interaction micro-
scopic calculations discussed in the text. A pure $(1f_{7/2})^{-2}$
configuration is assumed for the mass-54 states; two-
particle $(2p, 1f)$ configuration wave functions are used
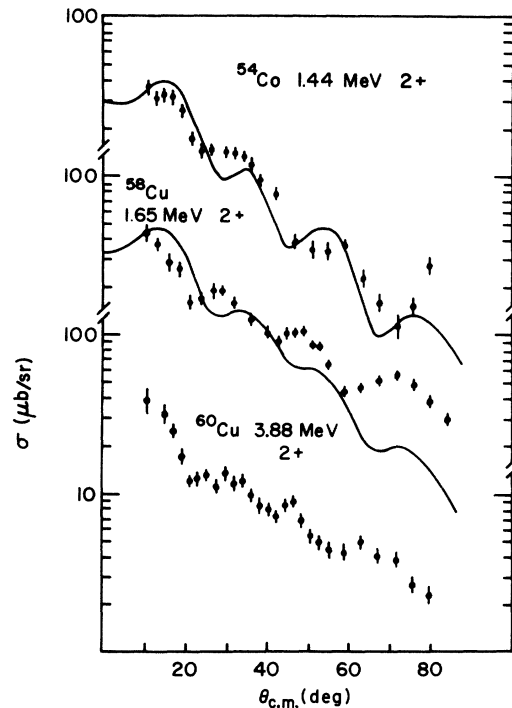for mass-58 states.

FIG. 5. $(^3$He, $t)$ angular distributions for three 2^+ iso-
baric analogs. The $L = 2$ curves result from the micro-
scopic calculations discussed in the text and outlined in
the Fig. 4 caption.

with this shape. The fact that only the analog state $L = 0$ transitions are detected experimentally is consistent with the DWBA calculations which predict approximately the same strength for all $p_{3/2}$, $f_{5/2}$, and $p_{1/2}$ in-shell $L = 0$ transitions. Only the ground-state analog transition contains completely constructive contributions from all subshells; the other 0^+ states have small cross sections due to their orthogonality to the ground-state analog.

The 2^+ first excited state analogs are identified primarily by their excitations relative to the ground-state analogs, which differ by less than 30 keV compared to the excitations of the parent states. The similar angular distributions for these states (Fig. 5) are characterized by pure $L = 2$ angular momentum transfer. High-resolution ($p, n\gamma$) data[14, 15] show that two states at 1.647 and 1.652 MeV lie within the interval spanned by the triton peak at 1.65 MeV. From the spectrum of ^{58}Ni the 2^+ $T = 1$ analog in ^{58}Cu is expected at about 1.65 MeV; the γ-ray decay modes imply[14] the analog is the higher member of the doublet. The present angular-distribution data suggest the $T = 1$ present state is preferentially populated. Angular

distributions for the ^{58}Cu 1.43-MeV state and for the ^{60}Cu ground state (Fig. 6) also appear to be characterized by $L = 2$ transfer. The spin of the ^{60}Cu ground state is known from atomic-beam experiments.[10] Although the spin-parity of the ^{58}Cu 1.43-MeV state is unknown, the similarity of the angular distribution to known pure $L = 2$ transitions suggest the state has $J^\pi = 2^+$. This state undergoes γ decay only to the ground state which is consistent with $J = 2$.[14, 15] We tentatively identify it with the 2^+, $T = 0$ state calculated at about this excitation (see Fig. 12).

The angular distribution of the ^{54}Co 2.63-MeV 4^+ analog state (Fig. 7) is indicative of $L = 4$ orbital angular momentum transfer. It is similar in structure to the angular distributions for the ^{54}Co 2.26-MeV state and the ^{58}Cu 2.69-MeV state. No other evidence exists to support a spin-parity assignment for the former state; however, the state in ^{58}Cu is assumed to be the 4^+ analog, since its excitation energy relative to the ground-state analog is within 20 keV of the excitation of the 4^+ parent state in ^{58}Ni.

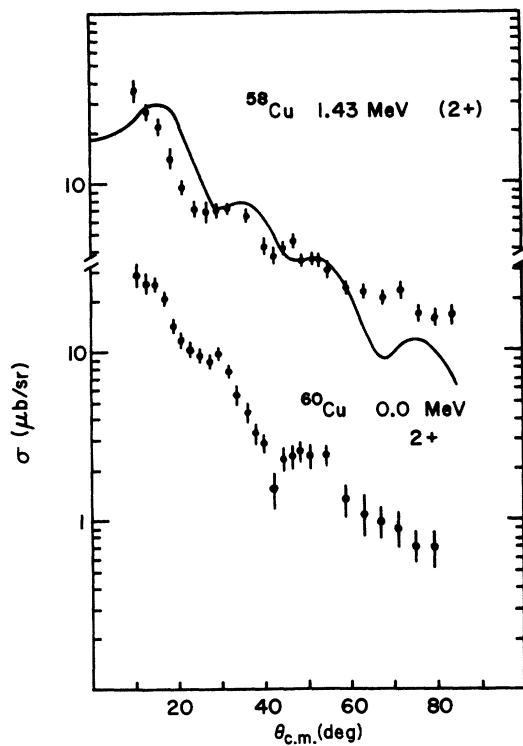Known and probable unnatural-parity transitions are shown in Figs. 8–11. The angular distribu-

FIG. 6. Angular distributions for the ^{60}Cu 2^+ ground state and the ^{58}Cu 1.43-MeV state. On the basis of the $L = 2$ shape, the latter state is tentatively assigned $J^\pi = 2$ as discussed in the text. The curve comes from calculations outlined in the Fig. 4 caption.
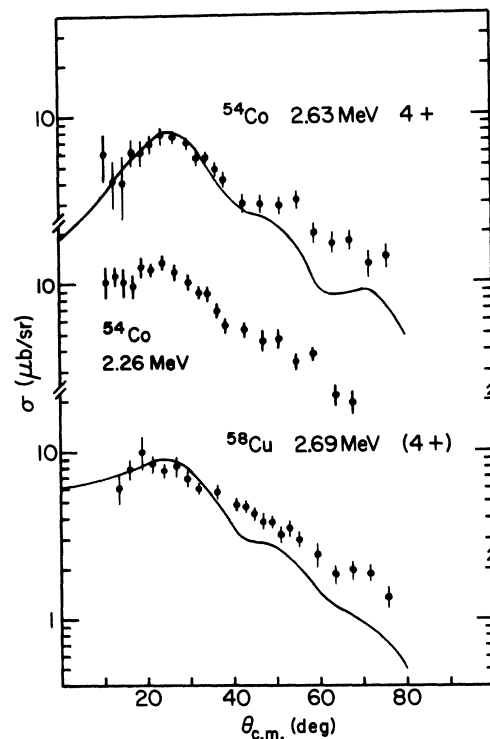

FIG. 7. Angular distributions for the 2.63-MeV ^{54}Co and 2.69-MeV ^{58}Cu 4^+ isobaric analog states. The $L = 4$ curves are calculated as outlined in the Fig. 4 caption. The 2.26-MeV ^{54}Co shape is similar but the spin of this state is unknown.

tions of the 0.94-MeV 1[+] state of [54]Co and the other three states shown in Fig. 8 appear to be incoherent mixtures of $L = 0$ and $L = 2$, with the latter angular momentum transfer dominant. The lifetime and γ-decay modes establish[14] $J = 1$ for the [58]Cu 1.05-MeV state; the triton angular distribution implies $J^{\pi} = 1^+$. The 1.78- and 2.18-MeV states of [60]Cu shown in the figure are populated in the $(^3\text{He}, p)$ reaction[11] with $L = 0 + 2$ and $L = 2$ transfers, respectively. This, together with the present data suggests the states have $J^{\pi} = 1^+$ and $(1, 2)^+$, respectively.

The data shown in Fig. 8 are consistent with the work of Bruge et al.[1] concerning the J dependence for unnatural-parity states where the angular distributions look more like those due to the higher rather than the lower possible orbital angular
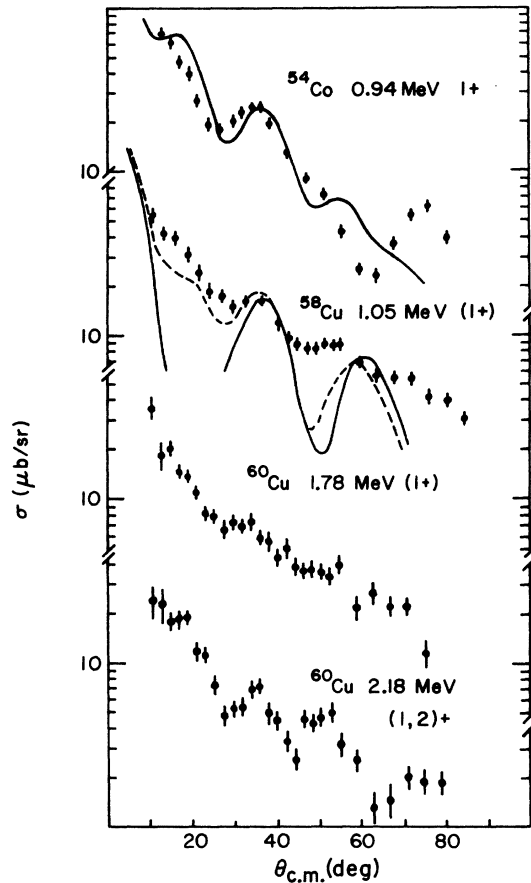
momentum transfer. However, the shapes of three other 0^+ to 1^+ transitions observed in this experiment (Fig. 9) do not follow this pattern and seem to be dominated by the lower possible angular momentum transfer $(L = 0)$. For two of these states, the [58]Cu ground state and the [60]Cu 0.06-MeV first excited state, there is conclusive evidence of 1^+ spin-parity assignments.[10, 20, 21] Positive evidence exists for the same assignment for the [60]Cu 0.67-MeV state, since this state is populated via $L = 0 + 2$ transfer in the $(^3\text{He}, p)$ reaction.

The angular distributions for the [54]Co 1.82-MeV state, the [58]Cu 0.45-MeV state, and for two states in [60]Cu at 0.45 and 0.90 MeV (Fig. 10) have the approximate appearance of combinations of $L = 2 + 4$ transfer. The [60]Cu 0.45-MeV state is populated by $L = 2 + 4$ transfer in the $(^3\text{He}, p)$ reaction which

FIG. 8. Angular distributions for states thought to have $J^{\pi} = 1^+$ as discussed in the text. These shapes are predominantly $L = 2$ in character. The curves result from microscopic calculations including a tensor interaction using pure $(1f_{7/2})^{-2}$ wave functions for [54]Co and the [58]Cu two-particle wave functions of Phillips-Jackson (solid curve), or Towner (dashed curve) (Refs. 10 and 27, respectively).
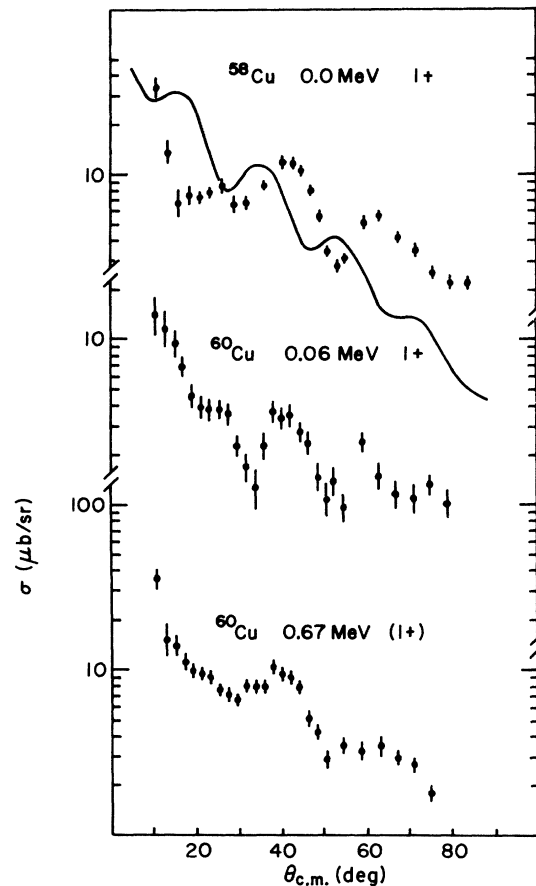

FIG. 9. Angular distributions with predominant $L = 0$ character for states known or thought to have $J^{\pi} = 1^+$. The curve is based on calculations outlined in the Fig. 8 caption. Both sets of wave functions give the same angular-distribution shape.

implies $J^\pi = 3^+$. The ^{58}Cu 0.45-MeV and ^{60}Cu 0.90-MeV states are tentatively assigned $J^\pi = 3^+$ due to the similarity of the angular distribution shapes; this is consistent with the γ-decay modes of both states.[14, 15, 17]

A state in ^{58}Cu at 2.94 MeV is populated in the (^{3}He, t) reaction with strength equivalent to the strong transitions to states below 2 MeV excitation. The angular distribution for this state shown in Fig. 11 (compare with the angular distributions for the 5^+, 6^+, and 7^+ states in ^{54}Co) is characteristic of a large angular momentum transfer and is most similar in shape to the ^{54}Co 5^+ angular distribution. $J = 5$ is the largest spin expected for states strongly populated in the (^{3}He, t) reaction considering the computed two-particle configurations of ^{58}Ni and ^{58}Cu. Results of calculations based on the assumption that this is the $(1f_{5/2})^2_{J=5}$ state are given below.

Figure 12 compares the energy levels and tentative spin assignments found here with the results from the (p, $n\gamma$) measurements and structure calculations of Phillips-Jackson.[10] The ^{60}Cu data given in Fig. 13 include results of this work, Ref. 10, and the (^{3}He, p) experiment.[11] The theoretical level scheme is taken from Ref. 10. The data from both copper isotopes are summarized in Tables I and II. The parentheses in the tabular data imply L and J^π assignments are based solely on assumed angular distribution systematics.

IV. MICROSCOPIC DISTORTED-WAVE ANALYSIS

The microscopic distorted-wave formalism has been discussed by Madsen[22] and Satchler.[23] The target may undergo any inelastic or quasi-inelastic excitation connected to the ground state by one-nucleon excitation. Since the amplitude for direct charge exchanged is proportional to the coherent sum over the shell-model terms of the charge-exchange nucleon, cross sections are expected to depend sensitively on wave-function admixtures. The nucleon-nucleon interaction responsible for
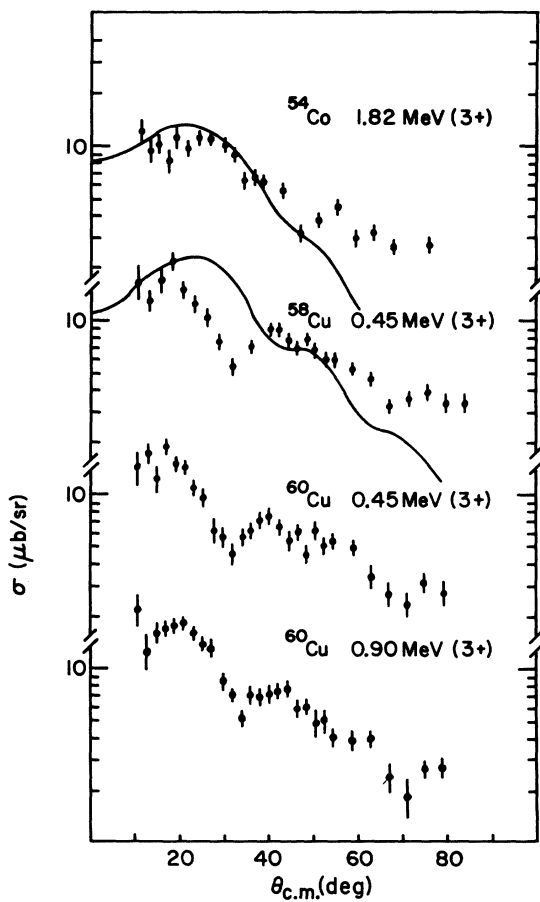

FIG. 10. Angular distributions for states thought to have $J^\pi = 3^+$ as discussed in the text. The curve comes from calculations outlined in the Fig. 8 caption. Both sets of wave functions give the same angular-distribution shape.
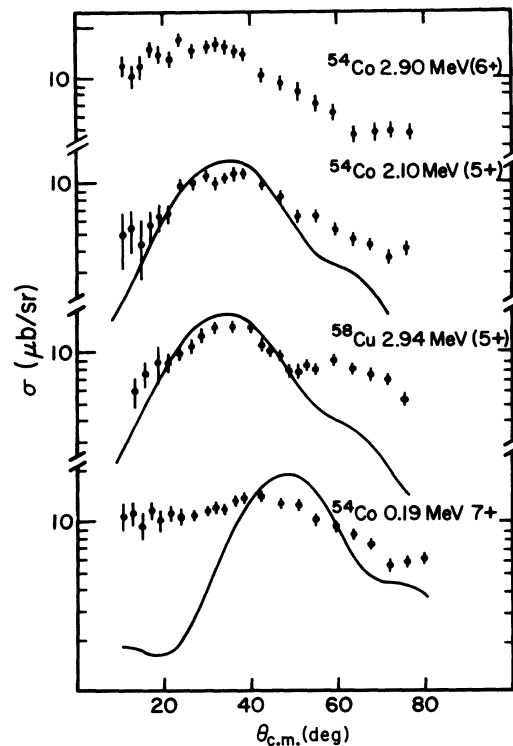

FIG. 11. Angular distributions for states with $J \ge 5$. The curves come from calculations outlined in the Fig. 8 caption. Both sets of wave functions give the same angular-distribution shape.

charge-exchange transitions is assumed to have the form

$$V(r) = \vec{\tau}_1 \cdot \vec{\tau}_2 [V_{01} g(r) + \vec{\sigma}_1 \cdot \vec{\sigma}_2 V_{11} f(r) + S_{12} V_T h(r)] .$$

The central interaction strengths $V_{ST} = V_{01}$ or V_{11} correspond to spin transfer zero or one ($S = 0$ or 1) and V_T is the tensor interaction strength. S_{12} is the usual spin-space OPEP operator. The function $h(r)$ may have either the OPEP form

$$h(r) = \frac{e^{-\alpha r}}{\alpha r [1 + 3/\alpha r + 3/(\alpha r)^2]}$$

or the so-called regularized OPEP form (ROPEP) used by Madsen[7,24] where $h(r) = h(\alpha r) - \beta^3/\alpha^3 h(\beta r)$. For $\beta > \alpha$ this functional form removes the r^{-3} singularity but has the OPEP form for large r. The latter form was used for the calculations given here and Yukawa shapes were used for the central interactions.

As pointed out in the introduction the calcula-

tions were performed with the intention of using the ^{54}Fe(^{3}He, t)^{54}Co reaction to "calibrate" the effective interaction strengths. The assumption that the initial and final states in this reaction correspond to the $(f_{7/2})^{-2}$ configuration is supported (for the $T = 1$ states) by $B(E2)$ values reported for the ^{54}Fe 6^+ to 4^+,[25] and 2^+ to 0^+ transitions.[25,26] Thus for given angular momentum transfer the strengths deduced from the mass-54 data ought to be similar to those required to fit the ^{58}Ni(^{3}He, t)^{58}Cu data provided the reaction model and mass-58 wave functions are correct. Two sets of wave functions were employed in the calculations. The first set, from Jackson,[10] uses empirical two-particle $T = 1$ and Kuo-Brown $T = 0$ matrix elements. The second set of Towner[27] is based on Kuo-Brown matrix elements. Both sets yield comparable eigenvalues (compare Fig. 12 with Ref. 14).

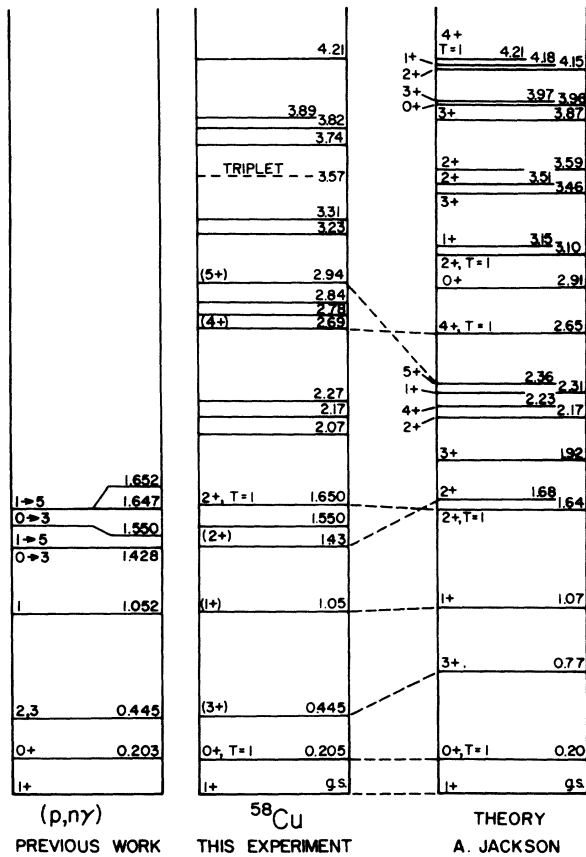In-shell transitions $((j)^2{}_{J=0} \rightarrow (j)^2{}_J)$ from a 0^+

FIG. 12. Energy level schemes for ^{58}Cu. The $(p, n\gamma)$ data are taken from Refs. 14 and 15. The present work suggests the spin-parity assignments and energy levels shown in the center diagram. The dashed lines indicate levels associated with the theoretical calculation (Ref. 10).
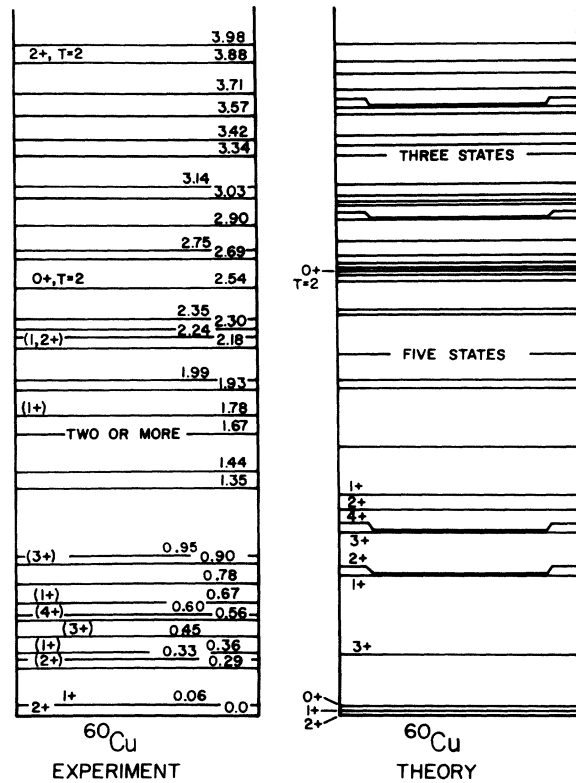

FIG. 13. Energy level schemes for ^{60}Cu. The experimental spin-parity assignments are based on the present work together with the results of Refs. 10, 11, and 21. The theoretical results are taken from Ref. 10.

target to natural-parity final states take place with zero spin transfer ($S = 0$), since the final states are antisymmetric in space-spin coordinates. Consequently, the ^{54}Fe(^{3}He, t)^{54}Co reaction to natural-parity states and the transition to the ground-state analog in ^{58}Cu are characterized by $S = 0$ and orbital angular momentum transfer (L) equal to J_f. The best choice for the inverse range parameter α of the central interaction V_{01} which determines these reactions is uncertain. The values 0.7, 1.0, and 1.2 fm^{-1} all have been used in the literature. For this reason test calculations were performed for the ^{54}Co 0^+ and 2^+ analog transitions where this parameter was varied in the range 0.5 to 1.5 fm^{-1}. Slight improvement in the fit for the 0^+ state was obtained for the larger values of α, while the 2^+ fit is slightly improved for smaller α. As a compromise the remainder of the calculations were performed with a central inverse range of 1.0 fm^{-1}.

Transitions to unnatural-parity states have $S = 1$ and $L = J_f \pm 1$. Reactions leading to $J > 0$ natural-parity states of ^{58}Cu may also have $S = 1$ contributions depending on the cross-shell to in-shell transition strengths. For $S = 1$ transfer, the V_{11} inverse range was also 1 fm^{-1}, and the ROPEP interaction parameters were $\alpha = 1$ fm^{-1} and $\beta = 4$ fm^{-1} in conformance with other analyses. No essential differences were found in trial calculations with $\beta = 2$ or 3 fm^{-1}.

The relative importance of the coherent tensor and central amplitudes for $S = 1$ transitions influence the importance of different projectile angular momentum transfers compared to λ, the orbital angular momentum transfer to the target nucleon. For tensor forces $L = \lambda$, $\lambda \pm 2$, and for central forces $L = \lambda$.[7, 24] Equal central and tensor strengths yielded the best angular distribution shapes for the 1^+ and 3^+ ^{54}Co states and these

relative strengths were used for the other transitions.

The potential well used to calculate the bound-state wave functions had the usual Woods-Saxon-plus-spin-orbit-plus-Coulomb-potential form. The Woods-Saxon radius and diffuseness parameters were 1.25 and 0.65 fm, respectively. The spin-orbit potential strength was chosen about 25 times the Thomas strength. The binding energy was determined by the separation-energy method. For example, for ^{58}Cu states:

$$E_{\text{binding}} = S_p - E_x + E_{\text{sp}}$$

where S_p is the proton separation energy, E_x the excitation energy of the state, and E_{sp} is the excitation of the passive neutron with respect to the ^{57}Ni ($p_{3/2}$) ground state. The calculated angular-distribution shapes were found to be insensitive to rather large variation of all the bound-state well parameters.

Three sets of optical-model parameters were investigated: a parameter set used previously in charge exchange calculations obtained by fitting ^{3}He elastic scattering on ^{62}Ni at 30 MeV[18]; an energy-dependent set used to fit ^{3}He + ^{58}Ni elastic scattering from 22 to 83 MeV[28]; and the 30-MeV ^{3}He + ^{62}Ni parameters together with triton parameters taken from the 20-MeV data of Hafele, Flynn, and Blair.[29] The last set gave an over-all better fit to the natural-parity states in ^{54}Co and was used in the rest of the analysis. The volume real and imaginary potential parameters for ^{3}He(t) were $V = 170.6$ MeV (151.3), $r_v = 1.143$ (1.24), $a_v = 0.712$ (0.678), $W = 18.5$ MeV (23.8), $r_w = 1.60$ (1.45), and $a_w = 0.929$ (0.841).

The distorted-wave calculations are in fair agreement with the ^{54}Co and ^{58}Cu natural-parity transition data shown in Figs. 4–7. While the theory reproduces the shape of the ^{58}Cu 2^+ transi-

TABLE III. Interaction strengths (MeV) from microscopic DWBA analysis.

(J,T) [a]	State (MeV)	^{54}Co $[(1f_{7/2})^{-2}]$	State (MeV)	^{58}Cu (P-J)	^{58}Cu (Towner)
(0, 1)	g.s.	64.9	0.20	65.1	76.5
(2, 1)	1.44	70.7	1.65	51.7	87.5
(4, 1)	2.63	98.4	2.69	74.5	77.1
(1, 0)	0.94	45.2	g.s.	12.5	16.1
(1, 0)			1.05	116	67.0
(3, 0)	1.82	17.8	0.45	12.4	17.8
(5, 0)	2.10	30.0	2.94	35.3	24.5
(7, 0)	0.19	45.7			
(2, 0)			1.43	134	192

[a] The strengths for $T = 1$ states correspond to $V_{ST} = V_{01}$ and the strengths for odd-J $T = 0$ states correspond to $V_{ST} = V_{11} = V_T$. The tabulated strength for the (2, 0) 1.43-MeV state assumes $V_{ST} = V_{01} = V_{11} = V_T$. (J,T) assignments are discussed in the text.

tions shown in Figs. 5 and 6, the 4° angular shift between theory and experiment is enigmatic, since no reasonable parameter variation removes the discrepancy. A similar effect has been noted for (^{3}He, t) reactions on ^{48}Ca and in the mass-90 region.[30] The calculations were normalized to the data by inspection as shown in the figures. The deduced interaction strengths are tabulated in Table III where comparisons between the Phillips-Jackson[10] (P-J) and Towner[27] ^{58}Cu wave functions are shown. While the ^{58}Cu strengths are roughly comparable to those found for ^{54}Co, particularly large differences are found for the 2^+ $T = 1$ ^{58}Cu state depending on the wave-function set. This is indicative of the extreme sensitivity of these calculations to small changes in configuration admixtures. The P-J or Towner calculations differ by only 90 keV in predicting the $0^+ - 2^+$ $T = 1$ energy separations.

The calculations predict comparable $S = 0$ and 1 contributions for the ^{58}Cu (2^+, $T = 0$) state, but very small $S = 1$ components for the 2^+ and 4^+ $T = 1$ states. For example, with $V_{01} = V_{11} = V_T$, less than 5% of the cross section comes from $S = 1$ transitions to these $T = 1$ states. The spin-transfer dependence on T arises from the phase relations between the configuration amplitudes $B_i(j_1 j_1)$ and $B_f^*(j_1 j_2)$ corresponding to the components $(j_1^2)J_i$ and $(j_1 j_2)_{J_f}$ of the initial and final wave functions. The spectroscopic amplitude for the (^{3}He, t) reaction on the 0^+ $T_i = 1$ target between these components is proportional[22] to

$$W(1\tfrac{1}{2} T_f \tfrac{1}{2}; \tfrac{1}{2}1)W(0 j_1 J_f j_2; j_1 J_f)B_i(j_1 j_1)B_f^*(j_1 j_2).$$

Since $B(j_1 j_2) = (-1)^{j_1 + j_2 - J - T}B(j_2 j_1)$, cross-shell spectroscopic amplitudes (associated with $S = 1$ transfer) such as $(p_{3/2})^2 - (p_{3/2}f_{5/2})$ and $(f_{5/2})^2 - (f_{5/2}p_{3/2})$ tend to add destructively for $T = 1$ states and add coherently for the $T = 0$ state. The small $S = 1$ contribution to the $T = 1$ states was ignored in establishing the potential strengths given in the table.

The unnatural-parity ^{54}Co cross sections are shown in Figs. 8, 10, and 11. As previously pointed out,[8] the tensor interaction favors the larger of $L = J_f \pm 1$ for in-shell transitions. Taking $V_{11} = V_T$, the ^{54}Co angular distributions shown in these figures reflect this fact. The associated interaction strengths listed in Table III are not constant, but approximately agree with the results Rost and Kunz[8] obtained by fitting 37.5-MeV (^{3}He, t) data.

The data for both the ground and 1.05-MeV 1^+ ^{58}Cu states are in poor agreement with our calculations. For either set of wave functions, not only do the predicted angular distributions have the wrong shapes, but the interaction strengths are drastically different than that found from the ^{54}Co

1^+ transition. Of the two, the Towner wave functions do yield a somewhat better angular-distribution shape for the ^{58}Cu 1.05-MeV transition shown in Fig. 8 and, indeed, somewhat more consistent interaction strengths. A comparison of the two ^{58}Cu structure calculations (compare Fig. 12 with Ref. 14), which predict essentially identical energy separation for the two 1^+ states, again indicates the extreme sensitivity of the charge-exchange model to small changes in magnitudes of various configurations. These transitions are also particularly sensitive to interaction-parameter variations, although no set of parameters simultaneously provides acceptable fits to both 1^+ states. The ^{58}Cu 1^+ ground state is predicted to have an $L = 2$ shape in contrast to the data shown in Fig. 9 which show large $L = 0$ strength. Madsen et al.[31] have discussed this particular transition and have shown that $1f_{7/2}$ core-polarization corrections to the two-particle wave functions bring the required interaction strength closer to agreement with other work. However, their computation also gives too much $L = 2$ strength.

The potential strength found for the 0.45-MeV ^{58}Cu (3^+) state is consistent with the ^{54}Co (3^+) data but the angular-distribution shape (Fig. 10) agrees only roughly with the data. Indeed incoherent superpositions of $L = 2 + 4$ shapes will not reproduce the experimental minimum at about 32°. Figure 11 shows the calculated shape for the ^{58}Cu 2.94-MeV state, assuming $J^\pi = 5^+$ as discussed above, along with 5^+ and 7^+ computations for ^{54}Co. The 5^+ interaction strengths given in Table III are in approximate agreement. Both the Phillips-Jackson and Towner wave functions predict essentially identical angular-distribution shapes for all the ^{58}Cu transitions except for the 1.05-MeV state discussed above.

V. SUMMARY

Spin assignments for several states in ^{58}Cu and ^{60}Cu are suggested on the basis of the apparent systematic J-transfer dependence of the (^{3}He, t) angular distributions. For the natural-parity final states, characteristic angular shapes imply the reaction mechanism is direct and that the associated selection rules are applicable. The interaction strengths obtained here for all ^{54}Co and the $T = 1$ ^{58}Cu states are larger than those found at higher incident energies,[8] but are consistent with a smooth dependence on ^{3}He energy found from analyses of data[32] at energies ranging from 21 to 37.5 MeV.

Several distinctive angular-distribution shapes are found for unnatural-parity final states as well. However, the situation is complicated compared to simple in-shell transitions (for example, ^{54}Fe

– ^{54}Co). From arguments based on corroborative (^{3}He, p), γ-decay, and atomic-beam measurements, two different shapes exist for 1^{+} transitions. In the same way, it is argued that 3^{+} transitions exhibit a distinctive shape. The microscopic DWBA calculations fail to reproduce these shapes or to yield consistent interaction strengths. It is unclear to what extent an inadequate reaction mechanism model for/or inaccurate wave functions cause these discrepancies. Indeed, for these transitions where the available wave functions predict important cross-shell transitions with $S = 1$, rather small configuration amplitude differences drastically influence the DWBA cross sections. In this context empirical systematics are somewhat surprising.

Papers published[14, 31, 33] after the present work was initiated have emphasized that the simple two-particle wave functions are not completely valid descriptions of these low-lying mass-58 states. In addition, several inadequacies of the Born-approximation reaction model have been pointed out. Examples are angular shifts of several degrees between DWBA calculations and the data,[30] the apparent breakdown of the model angular momentum selection rules for a few inhibited transitions,[34] and seemingly larger effective interaction strengths required to fit large angular momentum transfer transitions.[35] Schaeffer and Bertsch have shown[36] the last two effects are probably due to relatively important two-step processes. Despite these complications, systematics, such as those presented here, indicate further work may establish quantitative methods for doing (^{3}He, t) spectroscopy.

The authors wish to acknowledge and thank Professor V. A. Madsen for supplying a version of his DRC program.

---

[1]G. Bruge, A. Bussiere, H. Faraggi, P. Kossanyi-Demay, J. M. Loiseaux, P. Roussel, and L. Valentin, Nucl. Phys. A129, 417 (1969).

[2]R. C. Bearse, J. R. Comfort, J. P. Schiffer, M. M. Stautberg, and J. C. Stoltzfus, Bull. Am. Phys. Soc. 15, 574 (1970).

[3]H. Ohnuma, J. R. Erskine, J. P. Schiffer, J. A. Nolen, Jr., and N. Williams, Phys. Rev. C 1, 496 (1970).

[4]R. C. Bearse, J. R. Comfort, J. P. Schiffer, M. M. Stautberg, and J. C. Stoltzfus, Phys. Rev. Lett. 23, 864 (1969).

[5]J. J. Schwartz, R. Sherr, and T. Bhatia, Bull. Am. Phys. Soc. 13, 1446 (1968).

[6]J. J. Schwartz, Argonne National Laboratory Informal Report No. PHY-1970A, 1970 (unpublished).

[7]V. A. Madsen, Nuclear Isospin, edited by J. D. Anderson, S. D. Bloom, J. Cerny, and W. W. True (Academic, New York, 1969), p. 149, and references therein.

[8]E. Rost and P. D. Kunz, Phys. Lett. 30B, 231 (1969).

[9]R. Schaeffer, Nucl. Phys. A164, 145 (1971).

[10]E. A. Phillips and A. D. Jackson, Phys. Rev. 169, 917 (1968); A. D. Jackson, private communication.

[11]H. J. Young and J. Rapaport, Phys. Lett. 26B, 143 (1968).

[12]S. I. Warshaw, A. J. Buffa, J. B. Barengolta, and M. K. Brussell, Nucl. Phys. A121, 350 (1968).

[13]H. Rudolph, Ph.D. thesis, State University of New York at Stony Brook, 1970 (unpublished).

[14]D. F. H. Start, L. E. Carlson, D. A. Hutcheon, A. G. Robertson, E. K. Warburton, and J. J Weaver, Nucl. Phys. A193, 33 (1972).

[15]N. S. P. King, C. E. Moss, H. W. Baer, and R. A. Ristinen, Nucl. Phys. A177, 625 (1971).

[16]A. J. Cookson, Phys. Lett. 24B, 570 (1967).

[17]L. Birstein, C. Drory, A. A. Jaffe, and Y. Zioni, Nucl. Phys. A97, 203 (1967).

[18]S. I. Hayakawa, J. J. Kraushaar, P. D. Kunz, and E. Rost, Phys. Lett. 29B, 827 (1969).

[19]The 0^{+}, 2^{+}, 4^{+}, and 6^{+} assignments are based in part on the relative separation energies of these states compared to the ^{54}Fe parent states, as well as on earlier (^{3}He, t) angular-distribution data (Ref. 18). The probable 1^{+}, 3^{+}, 5^{+}, and 7^{+} assignments are based on γ-decay data (Ref. 15), as well as Ref. 18.

[20]E. J. Hoffman and D. G. Sarantites, Phys. Rev. 177, 1640 (1969).

[21]S. Cochavi, M. Marmor, and D. B. Fossan, Bull. Am. Phys. Soc. 15, 1681 (1970).

[22]V. A. Madsen, Nucl. Phys. 80, 177 (1966).

[23]G. R. Satchler, Nucl. Phys. 77, 481 (1966).

[24]C. Wong, J. D. Anderson, V. A. Madsen, R. A. Schmittroth, and M. J. Stomp, Phys. Rev. C 3, 1904 (1971).

[25]S. Cochavi, D. B. Fossan, S. H. Henson, D. E. Alburger, and E. K. Warburton, Phys. Rev. C 2, 2241 (1970).

[26]R. A. Ricci and R. R. Maurenzig, Rev. Nuovo Cimento 1, 291 (1969).

[27]I. Towner, private communication from E. K. Warburton.

[28]H. Chang and B. W. Ridley, Univ. of Colorado Report No. C00-536-653, 1970 (unpublished).

[29]C. F. Hafele, E. R. Flynn, and A. G. Blair, Phys. Rev. 155, 1238 (1967).

[30]J. R. Comfort, J. P. Schiffer, A. Richter, and M. M. Stautberg, Phys. Rev. Lett. 26, 1338 (1971).

[31]V. A. Madsen, V. R. Brown, F. D. Becchetti, and G. W. Greenlees, Phys. Rev. Lett. 26, 454 (1971).

[32]W. L. Fadner, H. Rudolph, and J. J. Kraushaar, Univ. of Colorado Report No. C00-535-674, 1972 (unpublished).

[33]L. E. Carlson, D. A. Hutcheon, A. G. Robertson, D. F. H. Start, E. K. Warburton, and J. J. Weaver, Nucl. Phys. A162, 35 (1971).

[34]R. A. Hinrichs, R. Sherr, G. M. Crawley, and I. Proctor, Phys. Rev. Lett. 25, 829 (1970).

[35]R. Schaeffer, Argonne National Laboratory Informal Report No. PHY-1970A, 1970 (unpublished).

[36]R. Schaeffer and G. F. Bertsch, Phys. Lett. 38B, 159 (1972).